

Proceeding Paper

Air Temperature Measurement Using CMOS-SOI-MEMS Sensor Dubbed Digital TMOS †

Moshe Avraham, Harel Yadid, Tanya Blank and Yael Nemirovsky *

Electrical and Computer Engineering Department, Technion – Israel Institute of Technology, Haifa 3200003, Israel; smoa@technion.ac.il (M.A.); harel.yadid@campus.technion.ac.il (H.Y.); tblank@technion.ac.il (T.B.)

* Correspondence: nemirov@ee.technion.ac.il

† Presented at the 9th Electronic Conference on Sensors and Applications, 1–15 November 2022; Available online: <https://ecsa-9.sciforum.net/>.

Abstract: Air temperature is an important meteorological parameter and is used for numerous purposes. Air temperature is usually observed using a radiation shield with ventilation, to obtain proper measurements by providing shade from direct solar radiation and increasing the heat exchange between the sensor and atmosphere. In rural areas, such auxiliary equipment is not available and it is still a challenge to obtain the air temperature accurately without aspiration. In this study, we describe a novel qualified CMOS-MEMS low-cost sensor, dubbed Digital TMOS, for remote temperature sensing of air temperature. The novel key ideas of this study are (i) the use of the Digital-TMOS, (ii) a narrow optical band pass filter (4.26 μm \pm 90 nm) corresponding to the CO₂ carbon dioxide absorption band; (iii) measuring simultaneously the weather parameters.

Keywords: air temperature; remote sensing; thermal sensor; CMOS

1. Introduction

Air temperature sensors and methods of measurement have been reported in several recent articles. All the papers describe the importance and challenges of air temperature measurement [1–4].

Air temperature is an important meteorological factor, which has a wide range of applications in fields like human health, virus propagation, growth and reproduction of plants, climate change, and hydrology. The WEB offers many types of thermometers for air temperature measurement, see for example [3].

What this report forgot to explain is that such thermometers cannot measure air temperature accurately since the measurement of air temperature is strongly influenced by environmental factors. Such as, humidity, solar radiation/duration, solar altitude angle, wind speed/direction, rainfall, atmospheric pressure, and other objects within the field of view. These factors make air temperature measurement very challenging. These issues become more pronounced in low-cost air temperature sensors, which lack a radiation shield or a forced aspiration system, exposing them to direct sunlight and condensation.

Air temperature is often observed using a radiation shield with ventilation to obtain proper measurements by providing shade from direct solar radiation and increasing the heat exchange between the sensor and atmosphere, thereby reducing error due to solar radiation incident on the sensor surface. Although a power-saving type shield that is driven by solar panels has been developed [4], many products still require mains power. However, mains power is not always available in rural areas, such as areas of farmland and forest. Meanwhile, recent studies have found strong contributions of the local background climate to the air temperatures observed at urban weather stations and these temperatures are sometimes different from those of nearby rural areas. It is thus important to

Citation: Avraham, M.; Yadid, H.; Blank, T.; Nemirovsky, Y. Air Temperature Measurement Using CMOS-SOI-MEMS Sensor Dubbed Digital TMOS. *Eng. Proc.* **2022**, *4*, x. <https://doi.org/10.3390/xxxxx>

Academic Editor: Francisco Falcone

Published: 1 November 2022

Publisher's Note: MDPI stays neutral with regard to jurisdictional claims in published maps and institutional affiliations.



Copyright: © 2022 by the authors. Submitted for possible open access publication under the terms and conditions of the Creative Commons Attribution (CC BY) license (<https://creativecommons.org/licenses/by/4.0/>).

observe the air temperature more easily in rural areas, and it has long been a challenge to obtain the air temperature accurately without aspiration.

In this study, we describe air temperature measurement, using a novel qualified CMOS-MEMS low-cost sensor, dubbed Digital TMOS, for remote temperature sensing of air temperature. The novel key idea of this study is the use of a narrow optical bandpass filter (4.26 μm \pm 90 nm) corresponding to the CO₂ carbon dioxide absorption band, on top of the Digital TMOS.

2. The Digital Thermal Device for Remote Temperature Sensing—Dubbed TMOS

The Digital TMOS has been described in several recent publications [5–8]. It is also reported in STM catalog [9]. The TMOS, short for Thermal-MOS, is thermal sensor based on thermally insulated MOSFET transistor. The TMOS is achieved by CMOS-SOI and MEMS process.

The Digital TMOS is described in Figure 1 below:

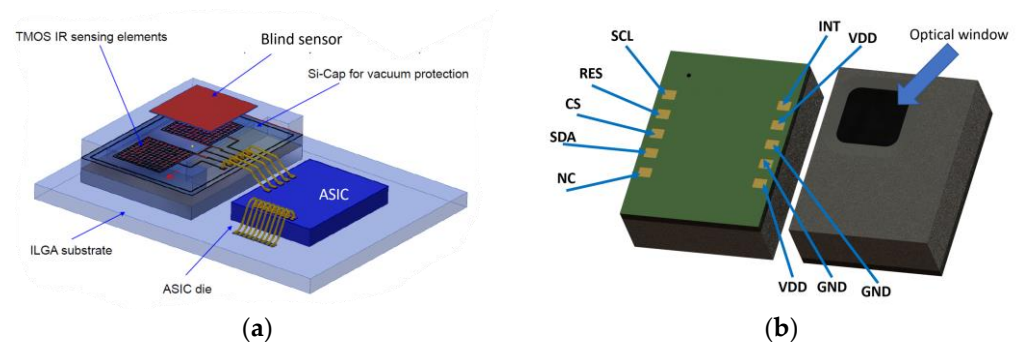


Figure 1. (a) Schematic description of the digital TMOS; (b) Organic LGA Package with SMD mounting (4.2 mm \times 3.2 mm).

The sample tailored to air temperature measurements contains two Digital TMOS's units, each TMOS is covered with an optical filter, of 4.26 μm \pm 90 nm (see Figure 2).



Figure 2. Image of the DUT sample (a) with two sensors; (b) packaged within a metal tube.

The reason we are using two Digital TMOS is to prove the following: The readings of the sensors are changing very rapidly. We assume that if the variations are due to the environmental changes, the readings of the sensors will be in correlation. In contrast, if the changes are due to sensor instability, there will be no correlation. This measurement is required to validate the results.

3. The Role of the Narrow Bandpass Optical Filter around 4.26 μm

It is well established that remote sensing of temperature, requires that the measured object will behave like a blackbody with known emissivity. The air emissivity is reported in [11]. The air is transparent to the visible and NIR radiation. CO₂ is always present in

the atmosphere as a greenhouse gas, with at least 400 PPM concentration. The CO₂ in the atmosphere absorbs the 4.26 μm radiation within an optical path of ~20 m. Hence, at this wavelength, the air may be treated like a blackbody with emissivity close to 1.

The Digital TMOS with the CO₂ filter is first calibrated with a blackbody [12] in the range of 0–100 °C and then it is ready to measure air temperature.

According to Planck's law, for a certain wavelength λ , at temperature T , the radiation power is as follows:

$$W(\lambda, T) = \frac{2\pi hc^2}{\lambda^5} \cdot \frac{1}{\exp\left(\frac{hc}{\lambda kT}\right) - 1} \left[\frac{\text{Watt}}{\text{cm}^2 \mu\text{m}} \right] \quad (1)$$

where c is the velocity of light, h is Planck's constant, and k is Boltzmann's constant.

Since we assume that the air temperature T_{air} is equivalent to the blackbody temperature T_{BB} , at 4.26 μm, we can rewrite the equation for a spectral measurement as:

$$W_{\lambda_1-\lambda_2}(T_{BB}) = W_{\lambda_1-\lambda_2}(T_{air}) = \int_{\lambda_1}^{\lambda_2} W_{\lambda}(\lambda, T_{air}) d\lambda \quad (2)$$

where in our case the wavelength spectrum [λ_1 , λ_2] is the CO₂ filter's optical band pass 4.26 μm ± 0.09 μm.

The radiation, measured by the Digital TMOS, is given by:

$$\begin{aligned} P_{\lambda_1-\lambda_2}(T_{air}) &= \varepsilon_{air} \cdot A_D \cdot W_{\lambda_1-\lambda_2}(T_{air}) \cdot \sin^2\left(\frac{\theta}{2}\right) \cdot t_{filter} \cdot \eta \\ &= \varepsilon_{air} \cdot W_{\lambda_1-\lambda_2}(T_{air}) \cdot \left[\underbrace{A_D \cdot \sin^2\left(\frac{\theta}{2}\right) \cdot t_{filter} \cdot \eta}_{PTF} \right] \end{aligned} \quad (3)$$

In case of a conic view of the detector, the solid angle will be summed across the field of view:

$$\text{Power Transfer Function} = PTF = A_D \cdot \sin^2\left(\frac{\theta}{2}\right) \cdot t_{filter} \cdot \eta \quad (4)$$

where A_D is the detector area, t_{filter} is the transmission factor of the filter, θ is the field of view (FOV) angle and η is the absorption coefficient.

The total absorbed radiation by the digital sensor is:

$$\begin{aligned} P_{\lambda_1-\lambda_2}(\varepsilon, T_{air}, T_{amb}) \\ = PTF \cdot \varepsilon_{air} W_{\lambda_1-\lambda_2}(T_{air}) + PTF \cdot (1 - \varepsilon_{air}) \cdot W_{\lambda_1-\lambda_2}(T_{amb}) \end{aligned} \quad (5)$$

The second term on the right side is the reflected power that the detector senses and it is determined by the objects around the sensor, such as the earth. Obviously, with air emissivity close to 1, this term becomes less significant.

The Digital TMOS measures the incident radiation (Equation (5)) and by applying the calibration algorithm of the sensor, the air temperature is obtained.

4. Measurements Results

Our measurements are classified to two types of measurements:

1. measurements at nighttime at different view angles, made with a digital TMOS tailored to the application.
2. measurements at daytime with different scenarios.

4.1. Nighttime Measurements

The measurements were taken from a window view, around 6–8 m above ground, in three different angles. (i) A low angle with ground view where the sensor is looking downwards. (ii) A mid-angle with a horizontal view, the sensor is looking forwards. (iii) A high-

angle with sky view, the sensor is looking upwards. The setup view and the results for nighttime measurements are shown in Figure 5.

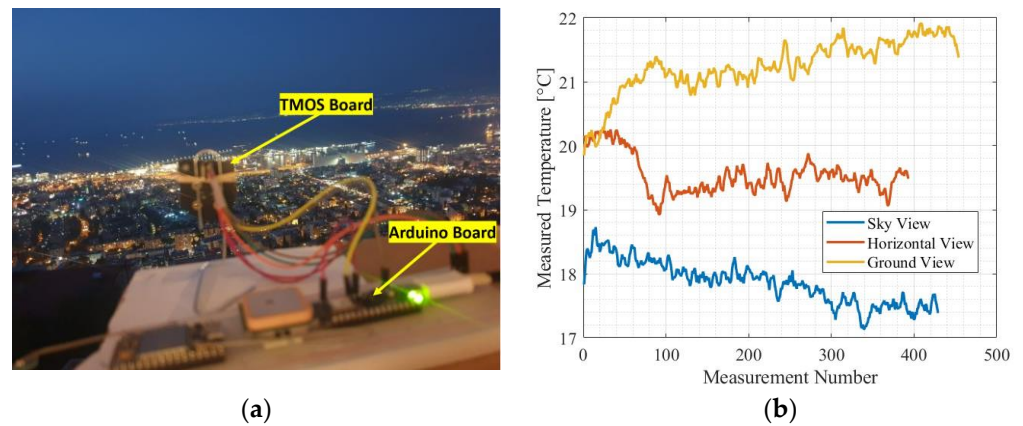


Figure 5. Nighttime measurements: (a) The front view of the Digital TMOS measurements at night; (b) The blue line indicates the Digital TMOS looking downwards, the red line indicates the Digital TMOS looking forwards, and the blue line indicates the Digital TMOS looking upwards.

From the results we can learn two interesting behaviors of the air temperature. First, the temperature changes rapidly. Second, the temperature changes with the view for obvious reasons, as explained below.

The heat capacity of the ground is larger than that of the air. Therefore, the ground is hotter than the air at nighttime. At the higher angle view, looking towards the sky, we measure the colder air temperature. At the lower angle of view, the ground is viewed by the sensor and the temperature is warmer. The horizontal view corresponds to the air temperature.

4.2. Daytime Measurements

We measured the air temperature with 3 detectors:

1. Digital-TMOS tailored to the application.
2. Sparkfun weather shield [13] with Si-7021 temperature/humidity detector [14].
3. RTD PT 100 connected to a USB adapter [15].

We took additional measurements of the relative humidity with the Si-7021 detector, the ambient light with an ALS-PT19 Sensor [16], and the barometric pressure with MPL3115A2 pressure sensor [17]. The measurements were taken in three different views—a corridor view, sunny view, and shadow view. The temperature results are as shown in Figure 6.

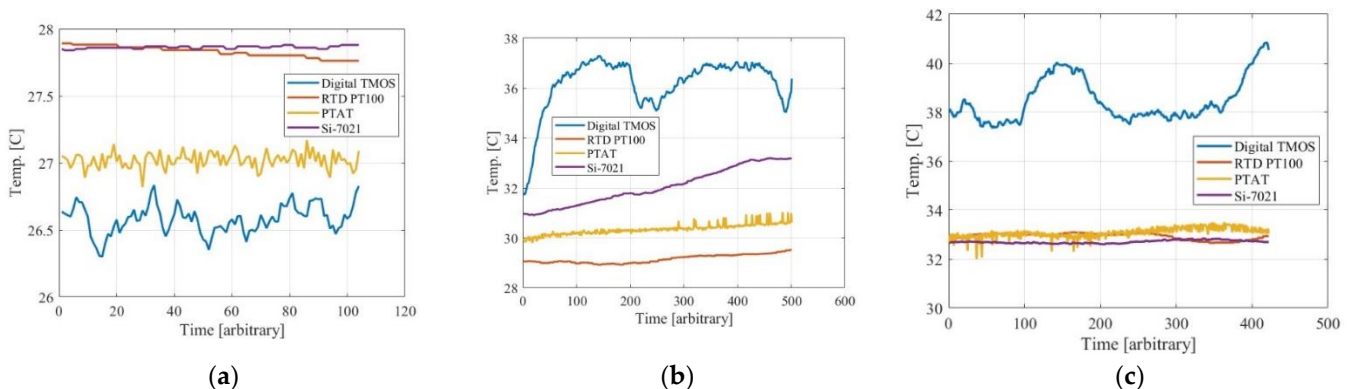


Figure 6. Three-temperature-detector measurement in 3 different views. The blue line indicates the Digital measurement, the red line indicates the RTD PT100 measurement, the yellow line indicates the PTAT measurement—equivalent to the digital TMOS board temperature, and the purple line indicates the Si-7021 measurement.

Figure 6a examines the results in a corridor indoor view. The Digital TMOS and the Si-7021 are standing together in the end of the corridor, viewing its full view. The RTD is standing 8 m inside the corridor, nearer to the entrance, measuring the temperature locally.

We can see in the corridor measurement that the Digital TMOS shows the coolest temperature. Since there is no sun in the corridor, we assume the main reason for the differences is air tunnels in the entrance of the corridor that lower the temperature in the far view from the digital TMOS location. Because of that we can also see strong fluctuations in the TMOS measurements.

Figure 6b examines the results in a sunny view, next to a rocky ground, where the digital TMOS is collecting data while standing in the shadow. The Si-7021 and the RTD PT100 are collecting data in the sun.

Figure 6c examines the results in a shadowy view, next to a rocky ground, where the digital TMOS is collecting data standing in the sun, and looking on a shadowed view. The Si-7021 measuring next to it, and the RTD PT100 are collecting data in the shadowed view. All measurements were taken in a two-minutes time.

As for the sunny view measurements, we can see that all the temperatures have risen in all the detectors. However, this time the Digital TMOS has shown the highest temperature, due to the rocky ground that was warmer than the air temperature. We can also see strong fluctuations that we will try to explain later. As for the other detectors, the Si-7021 has a linear change in the temperature due to heating in the sun, and the RTD PT100 is showing a stable temperature at the shadowed view.

In the shadow view measurement, the RTD PT-100 is exposed to the sun, and the Si-7021 changed location to the shadowed view. However, it took it much time to cool off. Compared to it, we can see the Digital TMOS measurements is a two-degrees higher but still with a strong fluctuation during the measurement.

Figure 7 exhibits the inverse correlation between the Digital TMOS and the measurement of the relative humidity. Assuming that the absolute humidity does not change during the short measurement time, it is obvious that if the temperature increases, the relative humidity is reduced and vice versa.

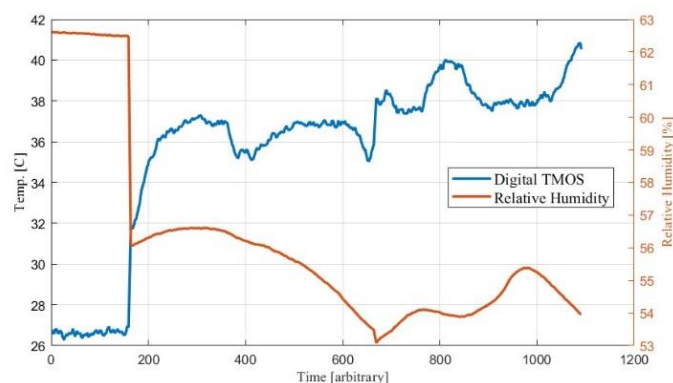


Figure 7. Digital TMOS temperature (blue) and Si-7021 relative humidity (red) measurements combined in all 3 views.

The measurements results are summarized below:

1. There is a strong and rapid connection between air temperature measurements derived from radiance power and the view we are measuring. We assume that it is due to rapid changes in the absolute humidity.
2. Landscape and earthly view have strong influence on the measurements. In order to receive most accurate measurements, the field of view should be narrow and the sensor should see just air.

5. Summary

Accurate air temperature measurement remains challenging, despite decades of research and development to improve instruments and methods.

Air temperature measurements are an essential component of weather monitoring and climate research worldwide and will continue to be challenging given the tradeoffs between accuracy, power consumption, and costs of the instrument options. With the advent of sensor technology and machine learning techniques, the performance of air temperature sensors will keep improving.

Author Contributions:

Funding: This research received no external funding.

Institutional Review Board Statement:

Informed Consent Statement:

Data Availability Statement:

Conflicts of Interest: The authors declare no conflict of interest.

References

1. Kim, S. Novel Air Temperature Measurement Using Midwave Hyperspectral Fourier Transform Infrared Imaging in the Carbon Dioxide Absorption Band. *Remote Sens.* **2020**, *12*, 1860. <https://doi.org/10.3390/rs12111860>.
2. Navarro-Serrano, F.; López-Moreno, J.I.; Azorin-Molina, C.; Buisán, S.; Domínguez-Castro, F.; Sanmiguel-Vallelado, A.; Alonso-González, E.; Khorchani, M. Air temperature measurements using autonomous self-recording dataloggers in mountainous and snow covered areas. *Atmos. Res.* **2019**, *224*, 168–179. <https://doi.org/10.1002/joc.4287>.
3. How Do You Measure Air Temperature Accurately? Available online: <https://www.nist.gov/how-do-you-measure-it/how-do-you-measure-air-temperature-accurately> (accessed on).
4. Blonquist, J.M., Jr.; Bugbee, B. Air Temperature. In *Agroclimatology*; Hatfield, J.L., Sivakumar, M.V., Prueger, J.H., Eds.; John Wiley & Sons.: Hoboken, NJ, USA, 2020. <https://doi.org/10.2134/agronmonogr60.2016.0012>.
5. Svetlitz, A.; Blank, T.; Stolyarova, S.; Brouk, I.; Shefi, S.B.; Nemirovsky, Y. CMOS-SOI-MEMS Thermal Antenna and Sensor for Uncooled THz Imaging. *IEEE Trans. Electron Dev.* **2016**, *63*, 1260–1265. <https://doi.org/10.1109/TED.2015.2513051>.
6. Zviagintsev, A.; Blank, T.; Brouk, I.; Bloom, I.; Nemirovsky, Y. Modeling the Performance of Nano Machined CMOS Transistors for Uncooled IR Sensing. *IEEE Trans. Electron Dev.* **2017**, *64*, 4657–4663. <https://doi.org/10.1109/TED.2017.2751681>.
7. Zviagintsev, A.; Brouk, I.; Bar-Lev, S.; Bloom, I.; Nemirovsky, Y. Modeling the Performance of Mosaic Uncooled Passive IR sensors in CMOS-SOI Technology. *IEEE Trans. Electron Dev.* **2018**, *65*, 4571–4576. <https://doi.org/10.1109/TED.2018.2863207>.
8. Blank, T.; Brouk, I.; Bar-Lev, S.; Amar, G.; Meimoun, E.; Meltsin, M.; Bouscher, S.; Vaiana, M.; Maierna, A.; Castagna, M.E.; Bruno, G.; Nemirovsky, Y. Non-Imaging Digital CMOS-SOI-MEMS Uncooled Passive Infra-Red Sensing Systems. *IEEE Sens.* **2020**, *21*, 3660–3668. <https://doi.org/10.1109/JSEN.2020.3022095>.
9. STMicroelectronics. Low-Power, high-Sensitivity Infrared Sensor for Presence and Motion Detection. 2022. Available online: https://www.st.com/content/st_com/en/products/mems-and-sensors/infrared-ir-sensors/sths34pf80.html#overview (accessed on).
10. Nanometric CMOS-SOI-NEMS transistor for uncooled THz sensing. *IEEE Trans. Electron Dev.* **2013**, *60*, 1575–1583. <https://doi.org/10.1109/TED.2013.2255293>.
11. SpectralCalc. High Resolution Spectral Modeling. 2022. Available online: <https://www.spectralcalc.com/info/about.php> (accessed on).
12. CI-Systems. SR-800N: Extended Area Blackbody. 2022. Available online: <https://www.ci-systems.com/sr-800n-superior-accuracy-blackbody> (accessed on).
13. Sparkfun. Sparkfun Weather Shield. Available online: <https://www.sparkfun.com/products/13956> (accessed on).
14. Silicon Labs. SI7021 Datasheet. Available online: <https://pdf1.alldatasheet.com/datasheetpdf/view/791426/SILABS/SI7021.html> (accessed on).

15. Dracal Technologies. RTD PT 100. Available online: https://www.dracal.com/en/products/?filters=product_cat%5brelative_humidity (accessed on).
16. Everlight. ALS-PT19 Ambient Light Sensor. Available online: https://cdn.sparkfun.com/assets/b/e/c/3/d/ALS-PT19_DS.pdf (accessed on).
17. MPL3115A2 Pressure Sensor. Available online: <https://www.nxp.com/docs/en/data-sheet/MPL3115A2.pdf> (accessed on).